

Next-Generation High-Strength Sheet Steel Utilizing Transformation-Induced Plasticity (TRIP) Effect

Yasuharu Sakuma*¹Atsushi Itami*²Osamu Kawano*²Noritoshi Kimura*¹Shunji Hiwatashi*²Kuniomi Sakata*³

Abstract:

An outline description is made of the elongation increase mechanism, manufacturing principles, production-line operating examples, formability, weldability, and fatigue strength of next-generation high-strength sheet steel utilizing the transformation-induced plasticity (TRIP) effect. Hot-rolled and cold-rolled sheets with tensile strengths of 590 to 980 N/mm² were produced from the next-generation high-strength TRIP steel and were proved to have a better combination of strength and elongation than conventional high-strength steels. The new high-strength TRIP steel was found to have very good stretchability near the plane-strain state and to yield high deep drawability in the TZP test. Since deformation on the punch shoulder occurs in the plane-strain state, TRIP increases the fracture strength, thereby improving the deep drawability of the steel. The spot weld strength of the new steel is comparable to that of conventional high-strength steels, and its fatigue strength is higher than that of dual-phase steel, which is claimed to have the highest fatigue strength for the same tensile strength.

1. Introduction

Automobiles that are industrial products must be low in manufacturing cost and running cost, not to mention high running performance. The strengthening of automotive sheet steels answers these functional requirements of automobiles and has been carried out with a view chiefly to improving fuel economy through weight reduction and enhancing passenger safety. Today, low production cost is given the top priority. The use of high-strength sheet steel with excellent formability comes in line with this primary objective, and brings the benefit of manufactur-

ing cost reduction through one-piece forming, for example. This article outlines the next-generation high-strength TRIP sheet steel with a tensile strength of 590 to 980 N/mm².

2. Application of TRIP to High-Strength Sheet Steel for Automotive Use

Transformation-induced plasticity (TRIP) refers to the phenomenon that austenite (γ), present in a chemically unstable condition, exhibits large elongation when it transforms to martensite with the addition of mechanical energy. The TRIP phenomenon is vividly observed in metastable austenitic stainless steel. Its stress-strain curve is shown in Fig. 1¹⁾. Unlike the deep drawing quality low-carbon steel for which relationship between the true

*1 Kimitsu Works

*2 Technical Development Bureau

*3 Oita Works

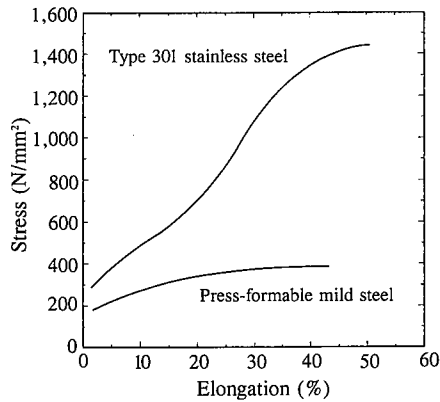


Fig. 1 Comparison of stress-strain curves of metastable austenitic stainless steel showing TRIP phenomenon and press-formable mild steel

stress σ and the true strain ε can be described by the n -th power hardening law

$$\sigma = K\varepsilon^n \quad \cdots(1)$$

the type 301 stainless steel exhibits an S shaped stress-strain curve. This is because the strength increase brought about by the strain-induced transformation of martensite adds to the simple work hardening of austenite. From a microscopic point of view, hardness is high enough to retard the deformation in the region where the transformation is completed, and deformation concentrates in the untransformed region. The occurrence and extension of necking are inhibited, with the result that uniform elongation increases.

Metastable austenitic stainless steel exhibits the TRIP phenomenon at room temperature, because the M_s temperature at which martensite transformation occurs on cooling is lower than room temperature and because nickel and carbon, for example, lower the free energy of austenite formation. The microstructure of deep drawing quality mild steel is made up of ferrite (α). Tensile strength of over 490 N/mm² needs precipitation strengthening or the presence of such a hard phase as martensite or bainite along with ferrite. Since low price is the first prerequisite, expensive alloying elements cannot be added to retain austenite as done for stainless steel. The effectiveness of TRIP²⁾ was recognized in the development of high-strength sheet steel with excellent formability but the knowledge could not be put to practical use for some time. This barrier was broken when silicon came to be utilized as alloying element and the continuous annealing and processing line (CAPL) was brought into operation where cooling from the recrystallization temperature is stopped at the overaging temperature³⁾. An alternative process also appeared that achieves the same effect for strip in the as-hot coiled condition by judiciously controlling the cooling of the strip on the runout table (ROT) of the hot strip mill⁴⁾.

The next-generation high-strength TRIP steel has the austenite phase stabilized by carbon enrichment⁵⁾. Its manufacturing principles are as illustrated in Fig. 2⁶⁾. When cold-rolled strip is processed on the CAPL, carbon and manganese concentrate in austenite through ferrite/austenite intercritical annealing, coupled with a ferrite growth during the subsequent slow cooling. When the ferrite is fully grown, the strip is cooled to the vicinity of 450°C at such a high rate that no pearlite is formed. Bainite transformation is then caused. Since silicon is contained and cementite formation is inhibited, carbon concentrates further in

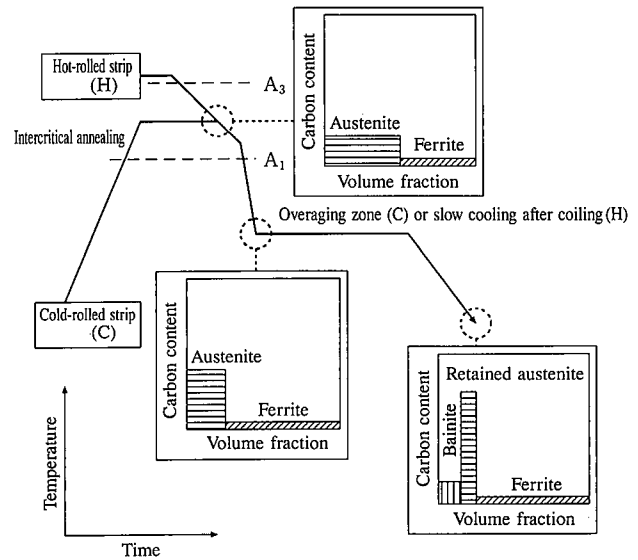
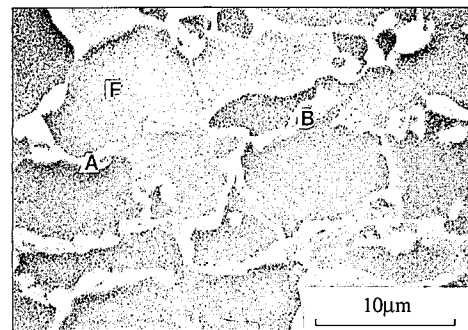


Fig. 2 Mechanism of retained austenite formation by carbon enrichment

untransformed austenite. As a result, the M_s temperature of the untransformed austenite falls below room temperature, and there is obtained the microstructure in which retained austenite (A) and bainite (B) are present together, centering on the grain boundaries of ferrite (F), as shown in Photo 1⁶⁾. When the sheet is formed at room temperature, the retained austenite transforms to martensite, bringing about the TRIP effect that expands the available forming range⁷⁾.

The next-generation high-strength TRIP steel is produced in the as-hot coiled condition as follows. To separate the microstructure into ferrite and austenite, the ferrite transformation is promoted by lowering the finish hot rolling temperature in one case. In another case, the steel is finish hot rolled under conventional conditions, rapidly cooled to refine the microstructure, and then slowly cooled until the ferrite transformation proceeds. In either case, the steel is rapidly cooled when the ferrite phase grows to such a level as to meet the target strength. The cooling is finished at a temperature above the bainite transformation region, and the strip is then coiled. The cooling finish temperature of dual-phase steel with martensite dispersed in the ferrite matrix is satisfactory if it is below the martensite transformation start temperature M_s . To leave the austenite phase in such an



A: Austenite, B: Bainite, F: Ferrite

Photo 1 Example of microstructure of next-generation high-strength TRIP sheet steel (590-N/mm² cold-rolled sheet, SEM image)

amount as to contribute to the TRIP effect, cooling must be completed in a certain temperature region. Some difficulty was thus encountered with the manufacture of the next-generation high-strength TRIP steel, but improving the operating technology made it possible to manufacture the steel with nearly the same stability as cold-rolled steels.

Table 1 summarizes the mechanical properties of next-generation high-strength TRIP steel sheets commercially produced upon these metallurgical principles. The strength-elongation balance of the TRIP sheets is compared with that of cold-rolled sheets in Fig. 3. The retained austenite volume fraction is about 6 to 10%, but the strength-elongation balance is much improved in the TRIP sheets.

3. TRIP Effect and Sheet Formability

It is well recognized that metastable austenitic stainless steel sheet that undergoes TRIP has excellent stretchability⁸⁾. The next-generation high-strength steel introduced here is presumed to have a similar effect, although the retained austenite volume fraction is small. Besides stretchability, there are deep drawability, stretch flangeability, and bendability as criteria to evaluate the sheet formability. The 1.0-mm thick 590-N/mm² cold-rolled steel (A), equivalent-strength precipitation-strengthened steel (P) and dual-phase steel (D), and equivalent-elongation phosphorus solid solution-strengthened steel (S), all listed in Table 2, were comparatively studied for formability. The results^{6,9,10)} are outlined below.

Stretchability was evaluated by limiting dome height (LDH) test with a 100-mm diameter spherical punch and hydraulic bulge test. Fig. 4 shows the results of stretchability close to plane

Table 2 Mechanical properties of next-generation high-strength TRIP sheet steel and conventional high-strength sheet steels

Steel	Yield point (N/mm ²)	Tensile strength (N/mm ²)	Total elongation (%)	(t = 1.0 mm)	
				n (5-15%)	\bar{r} (10%)
A: TRIP steel	339	614	35.0	0.244	0.86
P: Precipitation-strengthened steel	431	564	27.5	0.172	0.88
D: Dual-phase steel	346	653	27.0	0.185	0.70
S: Solid solution-strengthened steel	323	434	35.7	0.188	0.87

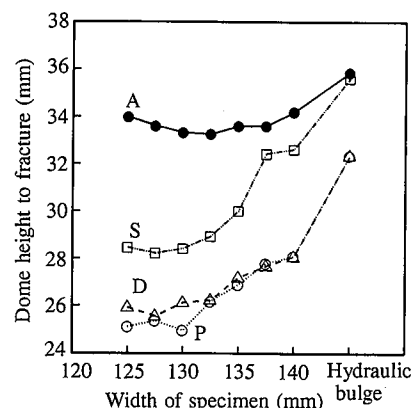


Fig. 4 Limiting dome height (LDH) in LDH test and hydraulic bulge test

strain as well as under balanced biaxial stretching as investigated by changing the width of 200-mm long specimens in the range of 125 to 140 mm. The limiting dome height of the TRIP steel A is superior to that of the equivalent-strength steels P and D, equal to that of the 440-N/mm² steel S in balanced biaxial stretching, and higher than that of the steel S close to plain strain. The limiting dome height is governed by the fracture limit strain and strain distribution. The present study reveals no differences in the fracture limit strain but shows differences in the strain distribution to be responsible for the difference of limiting dome height. Fig. 5 shows the strain distribution of the steel A in balanced biaxial stretching and plane-strain stretching. In deformation close to the plane strain state, the stress concentration is suppressed. The equivalent plastic strain at which diffuse necking occurs increases in the order of balanced biaxial stretching ($2n$), plane-strain stretching ($2n/\sqrt{3}$), and uniaxial stretching (n). The volume fraction of the retained austenite phase due to strain-induced transformation markedly decreases in the order of balanced biaxial stretching, plane-strain stretching, uniaxial stretching, and shrink flanging, as shown in Fig. 6. This is probably because the retained austenite phase that produces the TRIP effect and disperses the strain is present in a greater volume fraction in plane-strain stretching than in balanced biaxial stretching.

Next, deep drawability was measured by the TZP test using a 50-mm diameter cylindrical punch. The greater the T value of steel as calculated below, the higher the deep drawability the steel is judged to have in the TZP test. The T value is calculated as $(P_f - P_m)/P_f$, where P_f is the fracture load when the steel is forcibly fractured on the punch shoulder by constraining the flange under the blankholder force of 100 kN, and P_m is the maximum drawing load under the blankholder force of 10 kN. Fig. 7 shows the relationship between P_m , P_f , and tensile strength when the drawing ratio is 1.9. The TRIP steel A is large in P_f and slightly

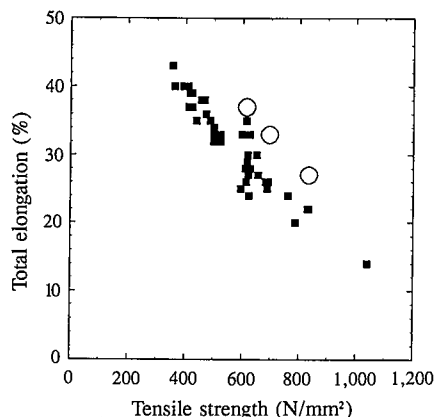


Fig. 3 Comparison of strength-ductility balance of sheet steels developed to date (■) and next-generation high-strength TRIP sheet steel (○)

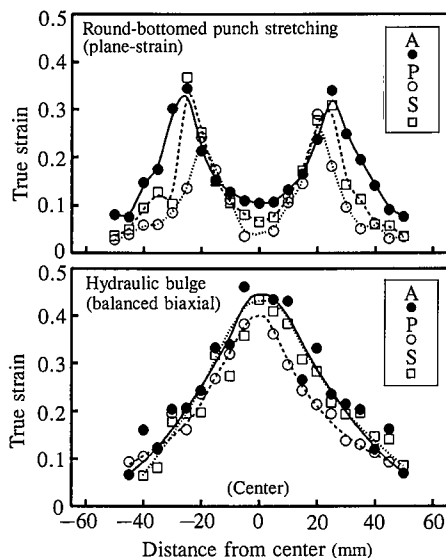


Fig. 5 Difference of strain distribution between plane-strain stretching and balanced biaxial stretching

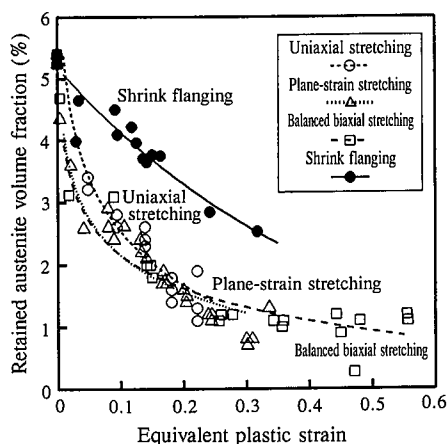


Fig. 6 Effect of difference of deformation mode on reduction of retained austenite phase due to work-induced transformation

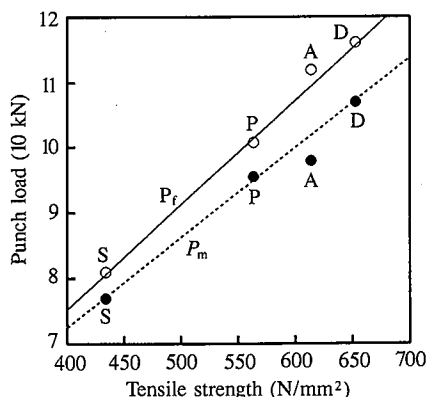


Fig. 7 Relationship of tensile strength with drawing load P_m and fracture load P_f at drawing ratio of 1.9

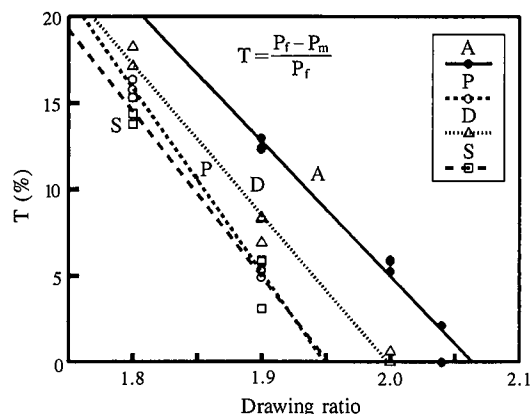


Fig. 8 Change of T value with drawing ratio

Table 3 Comparison of limiting draw ratio between next-generation high-strength hot-rolled TRIP sheet steel and conventional high-strength hot-rolled sheet steel

Steel	Thickness (mm)	Yield point (N/mm ²)	Tensile strength (N/mm ²)	Total elongation (%)	Limiting draw ratio
Next-generation high-strength hot-rolled TRIP steel	1.4	598	794	30	2.13
Conventional high-strength hot-rolled steel	1.4	510	617	24	2.13

small in P_m for its tensile strength, as compared with the other steels. The punch shoulder deformation is a plane-strain deformation, and increases P_f by the extent of hardening due to work-induced transformation. In shrink flanging, work-induced transformation is more difficult to cause and does not appreciably affect P_m . As a result, the next-generation high-strength steel A is large in the T value and superior in deep drawability as shown in Fig. 8, although its r value is small.

Hot-rolled sheet steels make use of the same strengthening mechanism as cold-rolled sheet steels do and have basically the same formability as the latter. As an example, Table 3¹¹⁾ shows the results of measurement of the limiting draw ratio (LDR). The LDR is the ratio of the blank diameter to the punch diameter at which the values of P_m and P_f obtained by the extrapolation method agree with each other in the TZP test. The 780-N/mm² next-generation high-strength TRIP steel has the same LDR as the conventional 590-N/mm² hot-rolled steel with a widened available forming range.

The above-mentioned results of small-size forming tests agree well with the results of model test with door panels formed on a large testing press. Fig. 9 shows the available forming ranges of the four sheet steels listed in Table 2.

From Fig. 9, it is recognizable that the conventional steels D and P cannot be formed into door panels, and that the TRIP steel A can be formed into door panels without wrinkling if the blankholder force is 1.5 MN or more. Forming with this large blankholder force also improves form fixability and is a key to prompting the strengthening of steel sheets that has not been attempted in the past for fear of increased springback.

4. Weldability and Fatigue Strength

Sheet steels are generally required to have high weldability to assemble stamped parts into automobiles. Setting aside arc welding, brazing and other sheet steel joining processes, here are

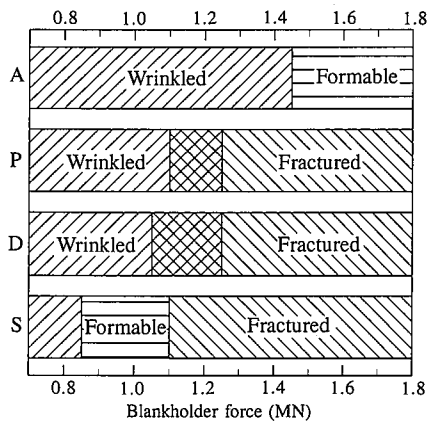


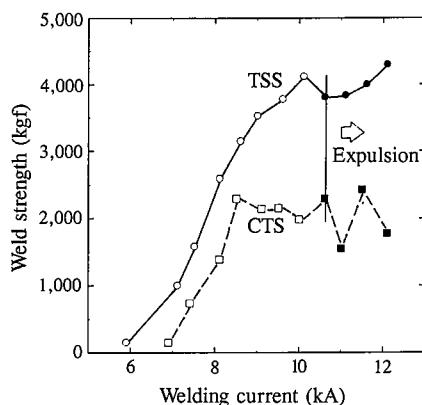
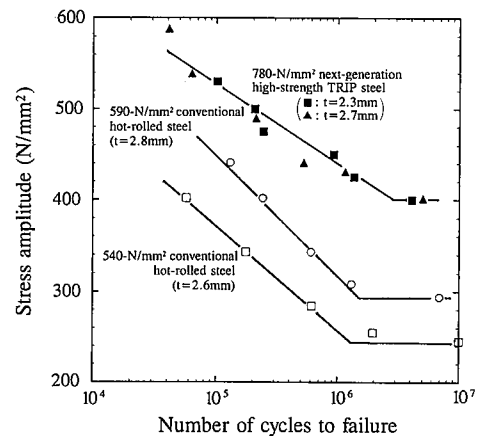
Fig. 9 Comparison of available forming range

introduced the results of investigation about spot weldability. Two 2.3-mm thick sheets of 780-N/mm² hot-rolled steel with mechanical properties as given in Table 4 were spot welded under the electrode force of 625 kgf using type CF electrodes of 8 mm diameter. Fig. 10 shows the change with the welding current in the tensile shear strength (TSS) and cross tension strength (CTS) of welds. Nuggets are formed when the welding current is 7 kA or higher, and the tensile shear strength and cross tension strength reach 4,100 and 2,200 kgf, respectively, when the welding current is 8.5 to 10 kA. When the welding current is 11 kA or higher, expulsion greatly varies the cross tension strength. The steel sheets listed in Table 1 are compositionally designed so as to fail outside of nuggets, so that they have weldability comparable to that of conventional high-strength steel sheets.

The service property primarily required of automotive sheet steels is corrosion resistance. Fatigue strength is the most important property required of undercarriage parts. The fatigue strength of dual-phase steel is higher than that of precipitation-

Table 4 Chemical composition (wt%) and mechanical properties of next-generation high-strength TRIP sheet steel used in weldability and fatigue strength tests

(t=2.3mm)								
C	Si	Mn	P	S	Al	Yield point (N/mm ²)	Tensile strength (N/mm ²)	Total elongation (%)
0.149	1.98	1.64	0.008	0.0012	0.028	568	821	31

Fig. 10 Weld strength of 780-N/mm² hot-rolled TRIP sheet steelFig. 11 Completely reversed plane bending fatigue test results of 780-N/mm² hot-rolled TRIP sheet steel

strengthened steel and bainitic steel. The fine cell structure formed in the initial cyclic hardening process is stable, and the strengthening of the ferrite phase by silicon and finely dispersed martensite retards the initiation and propagation of fatigue defects¹²⁾. Cyclic hardening refers to an increase in stress amplitude in strain-controlled fatigue testing. Cyclic hardening is also recognized when the retained austenite phase is included, and it is considered possible that a high stress field locally set up by fatigue may be relaxed by work-induced transformation¹³⁾. Fig. 11 shows the completely reversed plane bending fatigue test results of 2.7-mm thick sheets of the new 780-N/mm² hot-rolled steel and the conventional 540- to 590-N/mm² hot-rolled steels, as well as 2.3-mm sheets of the new high-strength sheet steel listed in Table 4. The 2×10^6 cycle fatigue strength of the high-strength TRIP steel is 400 N/mm², and is 1.4 to 1.5 times as high as that of the conventional steels with equal formability.

5. Conclusions

The microstructure of press-formed sheet steels, cold-rolled sheet steels, in particular, is predominantly made up of the ferrite phase alone, and their formability is governed by the texture of the ferrite phase and the amount and condition of microstructural impurities. Dual-phase steel with fine martensite dispersed in the ferrite matrix was developed to address this problem. The steel was intensively studied for practical use around 1980, but is not yet widely applied to automobile parts. The dual-phase microstructure, discovered as a new strengthening mechanism, has many advantages and disadvantages. Introduction of the retained austenite phase, a subject of heated pro and con arguments, is expected to encounter much difficulty. More than five years have passed since its manufacturability was first reported, and many excellent properties have been revealed from commercially produced sheet products. There are still many problems to be overcome, and this is one of the reasons for the term "next-generation" applied to this new class of sheet steel. We intend to find widespread use for this steel by solving its problems one after another.

References

- 1) Ludwigson, D.C., Berger, J.A.: J. Iron Steel Inst. 207, 63 (1969)
- 2) Goel, N.C., Sangal, S., Tangri, K.: Met. Trans. A. 16A, 2013 (1985)
- 3) Sakuma, Y., Matsumura, O., Takechi, H.: Met. Trans. A. 22A, 489 (1991)
- 4) Kawano, O., Haji, J., Easaka, K.: Am. Soc. Mecha. Eng. Prod. Eng. Div. 46, 11 (1991)
- 5) Sakuma, Y., Matlock, D.K., Krauss, G.: Met. Trans. A. 23A, 1221 (1992)
- 6) Hiwatashi, S., et al.: CAMP-ISIJ. 5, 1847 (1992)
- 7) Sakuma, Y., Matlock, D.K., Krauss, G.: Met. Trans. A. 23A, 1233 (1992)
- 8) Kawai, N., Saiki, H., Hirate, H.: J. Jpn. Soc. Technol. Plast. 17, 899 (1976)
- 9) Hiwatashi, S. et al.: Proceedings of 1993 Japanese Spring Conference for the Technology of Plasticity. 1993, p. 273
- 10) Katayama, T. et al.: SAE Technical Paper 920247. 1992
- 11) Ikenaga, N. et al.: Proceedings of Oita Local Meeting at Summer Meeting of Kyushu Chapter, Japan Society of Mechanical Engineers. 1992, p. 201
- 12) Mizui, M. et al.: J. of Soc. Mater. Sci. Jpn. 38, 15 (1989)
- 13) Takahashi, M., Mizui, M.: CAMP-ISIJ. 7, 756 (1994)